Journal of Materials Chemistry A

Accepted Manuscript

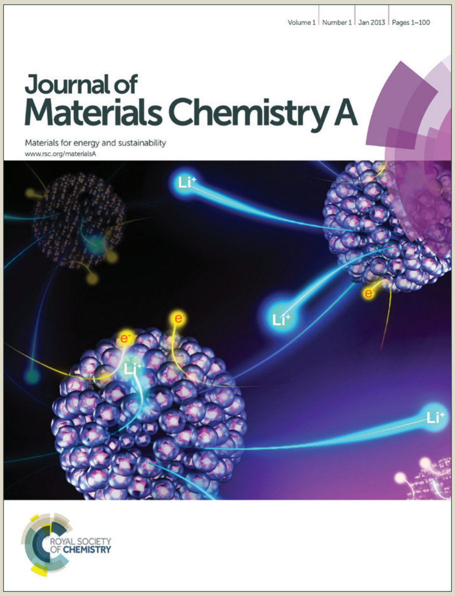

ROYAL SOCIETY OF CHEMISTRY

www.rsc.org/materialsA

Hierarchically macro/mesostructured porous copper oxide: Facile synthesis, Characterization, Catalytic performance and Electrochemical study of mesoporous copper oxide monoliths

Gowhar Ahmad Naikoo [a], Riyaz Ahmad Dar [b] and Farid Khan [a*]

[a]Nanomaterials discovery laboratory,
Department of chemistry,
Dr. Hari Singh Gour Central University, Sagar (M.P) 470003, India.
[b]Department of Chemistry,
University of Mumbai, Vidyanagari Santacruz (East)-Mumbai-400098, India

Corresponding author: - Farid khan

Designation: - Professor

Email id:-faridkhan58@yahoo.com

Phone: - +91-9425626334

Abstract

Hierarchically macro/meso structured porous copper-oxide monoliths with and without additives (dextran, 1, 3, 5-trimethylbenzene and silica nanoparticles) were successfully synthesized via facile Sol-Gel route and characterized by Scanning electron microscopy (SEM), Powder X-ray diffraction (PXRD), Thermagravimetric analysis (TGA), Brunauer-Emmet-Teller (BET) adsorption technique and FT-IR study. The results obtained reveal that the affect of additives have enhanced specific surface area from 0.558 m^2/g to 229.5 m^2/g and varied pore size from 8 μm to 39 nm are discussed. Furthermore, the hierarchically porous copper-oxide materials have shown excellent catalytic activity towards the wet oxidation of phenol and electrocatalytic performance of mesoporous copper oxide (mpCuO) against p-nitrophenol, demonstrating the significance of the porous nature of copper-oxide monoliths.

Keywords: Porous copper-oxide monoliths; Specific surface area; Catalytic activity; Electrochemical study

Introduction

Hierarchically porous materials with multiple-scale porous structure, generally micro-meso-macroporous, have attracted great attention recently due to their dynamic properties such as low density, considerable thermal conductivity,[1] gas permeability, bio-filtration capability,[2,3] and adsorption,[4,5] hence, such materials are extensively used in heterogeneous catalysis,[6-12] biosensor technology,[13,14] electrochemical supercapacitors,[15-18] tissue engineering,[19] photonic crystals, fuel cell electrodes,[12] and chemical separations.[2,3,20] So, the field of porous materials has been driven by a broad range of applications, many of which rely on the incorporation of specific guests into pores of different sizes and on the transport of such guests through the pores (e.g. catalysis, separations, sensing etc.).

Different methods, such as two-dimensional colloidal crystal template techniques,[21,22] aqueous chemical strategies,[23,24] chemical vapour deposition,[25,26] and hydrogen bubble dynamic template,[27] have been explored to fabricate the porous metallic nanostructures. But the controlled synthesis and characterization of porous inorganic materials is still a big challenge

In this work, macro/mesostructured porous copper oxide monoliths are successfully synthesized via facile Sol-Gel route. The influence of additives like dextran (2×10^{6} M), 1, 3, 5-trimethyl benzene (Mesitylene, TMB) and silica nanoparticles (Si-Nps, AS-40, colloidal silica, 40 wt% suspension in water, 20-25nm particle size) on the pore size, shape and thereby affecting the structure of the resulting porous nanostructures were investigated. Furthermore, the series of as synthesized porous copper-oxide materials were used for the first time as novel catalysts in the hydroxylation of phenol into dihydroxy phenols (catechol and hydroquinone) and mesoporous copper oxide (mpCuO) has shown excellent electrochemical performance towards the reduction of p-nitrophenol which has vast industrial and pharmaceutical importance. These findings expand the structural diversity of hierarchically porous copper-oxide materials for various innovative applications and novel properties through the self-assembly of amphiphilic surfactants with the metal precursor.

Experimental details

Chemicals and Materials

Copper nitrate trihydrate (Sigma Aldrich as a precursor), soft template Pluronic F-127, (Aldrich), structural directing agents like Dextran (Sigma Aldrich, 2×10^{6} M), 1, 3, 5-Trimethylbenzene (TMB, Merck), silica nanoparticles (Si-Nps, AS - 40, colloidal silica, 40 wt % suspension in water, 20-25 nm particle size, Sigma-Aldrich), were used as received.

Synthesis of hierarchically macro/mesostructured porous copper-oxide monoliths

Porous copper-oxide monoliths were prepared by dissolving 2.0 g $Cu(NO_3)_2.5H_20$ (50 wt%, Sigma-Aldrich) in 2.0 g of ultrapure water (50 wt%) and 2.0 g of Pluronic F-127 (14.81 wt%, M_w = 12,600, Aldrich) in 11.5 g of ultrapure water (85.19 wt%) at 25 $^{\circ}$C. The gel was heated for 1 h at 55 $^{\circ}$C on a magnetic stirrer to form the paste which gradually became light blue in colour. The resulting gel was aged for 2-3 days at room temperature and then calcined at 650 $^{\circ}$C for 2h at a heating rate of 1 $^{\circ}$C/min followed by cooling at a rate of 1°C/min to room temperature in an ELLITE furnace. CuO/Pluronic F-127/dextran, CuO/Pluronic F-127/TMB and CuO/Pluronic F-127/Si-NPs monoliths were prepared using the above protocol by adding 4.0 g dextran (57.14 wt%, M_w = 2×10^{6} M) in 3.0 g of ultrapure water (42.14 wt%), 2 g of 1,3,5 Trimethylbenzene (TMB) and 0.25 g of silica nanoparticles (Si-NPs, AS-40, colloidal silica, 40 wt% suspension in water) separately to Cu/Pluronic F-127 gel. The resulting gels were calcined at 650 $^{\circ}$C with the same heating and cooling rate.

Structure characterizations

Powder X-ray diffraction (PXRD) patterns of the calcined monoliths were obtained on a Bruker D-8 advance diffractometer in the diffraction angle range 2θ = 20-120°, using monochromatic Cu kα radiations ($\lambda = 1.541$). Examination of the morphology and pore diameter was carried out using a ZEISS microscope inbuilt with software operated at 20 KV. The Brunauer- Emmett- Teller (BET) surface area and pore volume of the porous CuO materials were determined by physisorption of N_2 at 77K over a Micromeritics ASAP 2010. The BJH method inbuilt in Micromeritics ASAP 2010 was used for measuring the pore diameter of the as synthesized samples. Perkin-Elmer thermal analyzer was used for thermal studies using alumina reference crucible at the heating rate of 10 °C/min. FT-IR studies were performed on Shimadzu-8400 spectrometer.

Catalytic activity

Hydroxylation of Phenol was carried out by a series of as synthesized porous copper-oxide materials in the presence of hydrogen peroxide (H_2O_2) to examine their catalytic performance. Catalytic reactions were run in a 250 ml glass reactor equipped with a reflux condenser and stirred with a magnetic stirrer at 50 °C.

In typical catalytic reactions, the molar ratio of Phenol to H_2O_2 was 1:1 with 1.0 g phenol (5.41 wt%) in 17.5 g ultrapure water (94.59 wt%), 0.05 grams (0.06 mole%) of as synthesized porous CuO materials with and without structural directing agents (dextran, TMB and Si-NPs) were used as catalysts and a time of 3.5 h for each successive catalytic reaction study. When reaction time was completed catalyst was removed by centrifugation and the composition of the products were analysed by HPLC technique. Shimadzu SPD - M 20A HPLC equipped with a reverse phase C18 column was used in the present study to investigate the product composition. Methanol/water mixture (30/70, volume ratio) was used as a mobile phase at a flow rate of 0.5 ml min^{-1} and detected at UV wavelength of 293 nm. The standard compounds (phenol, catechol, and hydroquinone) are used for identification and quantification of reactant and products.

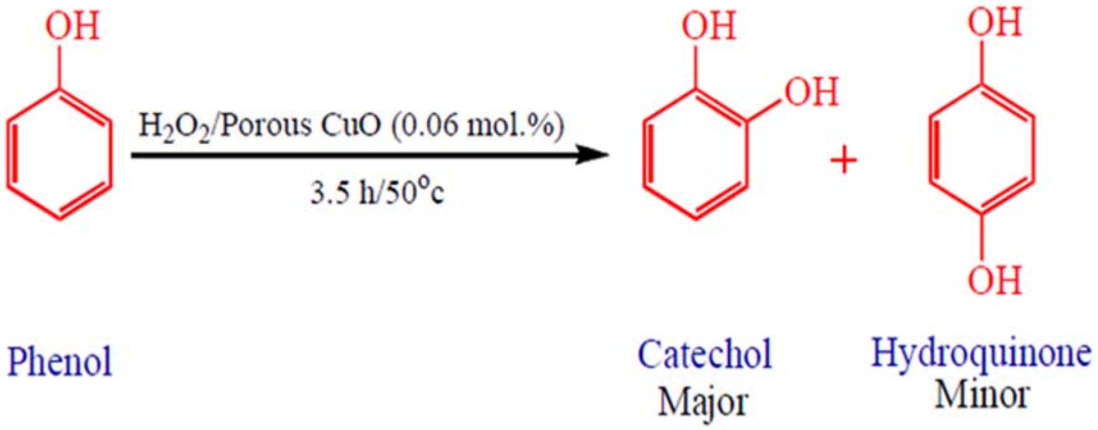

Electrochemical measurement of mesoporous copper oxide monoliths

All voltammetric experiments were performed with a CHI electrochemical workstation (CH Instruments Model CHI1100B series). Among the series of as synthesized porous copper-oxide monoliths, mesoporous CuO monoliths (CuO/F-127/Si-NPs) with highest surface area 229.5 m^2/g is used as a modifier for the electrochemical performance. The conventional three-electrode geometry was adopted. The working electrode was a mesoporous CuO modified glassy carbon electrode (mpCuO/GCE, 3 mm in diameter), the counter electrode was a platinum foil and the reference electrode was Ag/AgCl (in saturated KCl). 0.1 M KOH and saturated KCl solution was used as electrolyte for the two electrode electrochemical cell and for reference electrode cell respectively.

The obtained mesoporous CuO modified glassy carbon electrode (mpCuO/GCE) was prepared as follows: Initially, GCE was mechanically polished with 0.05 mm alumina slurry and then sequentially sonicated in dilute nitric acid, anhydrous ethanol and redistilled water for 15 minutes. Finally, the cleaned GCE was dried under nitrogen stream. Then after 5.0 mg mesoporous CuO materials were added to 2.5 mL ethanol solution, which was sonicated in ultrasound bath for 30 minutes to form a stable suspension. The mixed suspension of 10.0 µL was cast onto GCE surface by a micropipette, and then the suspension was thoroughly dried out under an infrared lamp. The electrode was rinsed by distilled water for several times and further dried in air before use, and the finally obtained electrode was denoted as mesoporous copper oxide modified glassy carbon electrode (mpCuO/GCE). For comparison, the bare GCE was used.

Results and discussion

PXRD and EDAX analysis

The composition and phase purity of the as-prepared products were examined by PXRD (Fig. 1), shows well-resolved peaks with reflections at d spacing's of 2.75, 2.52, 2.32, 1.86, 1.71, 1.58, 1.50, 1.41, 1.40, 1.30, 1.26, and 1.16 Å which correspond to (110), (002), (200), (-202), (020), (202), (-113), (022), (-311), (311), (004), and (312) lattice planes of a base-centred monoclinic unit cell (tenorite) crystal (JCPDS No.04.783). No impurity peaks were detected in the XRD pattern, indicating the formation of pure porous CuO materials under these experimental conditions. In case of porous CuO materials encapsulated with silica nanoparticles (CuO/F-127/Si-NPs), the identity was further established by EDAX (Fig. S1). It clearly exhibits the characteristic peaks of metallic Cu and silica, suggesting that the obtained product is encapsulated with silica nanoparticles.

SEM and BET sorption study

Fig. 2 gives panoramic SEM images of the macro/mesostructured porous CuO samples. The magnified image (Fig. 2) indicates that the typical morphologies of the as-prepared samples are hierarchically macro - mesostructured with the average pore diameter of about 8 µm (CuO/F-127, Fig. 2a), 780 nm, (CuO/F-127/Dextran, Fig. 2b), 830 nm (CuO/F-127/TMB, Fig. 2c) and 39 nm (CuO/F-127/Si-NPs, Fig. 2d). The clear view (Fig. 2d) reveals that silica nanoparticles are buried inside the porous CuO materials consistent with the EDAX results.

Pore size was increased when dextran or TMB was added to CuO/F-127 xerogels. We attribute this to changes in the viscosity of the composite gels and their rate of decomposition or solubilization of nonpolar TMB inside the surfactant assembly.[28,29] However, and the addition of silica nanoparticles to the gels reduced the pore size of these monoliths,[28-30] which suggests that other nanoparticles could also be used to fabricate the monoliths of desired architecture

For further study, N_2 sorption isotherms of the corresponding as synthesized macro/mesostructured samples are closely investigated. Among the series of as prepared monoliths porous CuO (CuO/F-127/Si-NPs) exhibit sorption isotherm of type 1V (Fig. 3) of the IUPAC classification featuring the mesoporous characteristics of the porous CuO materials.[31] The surface area of the hybrid materials shows a dramatic increase with the variation of structural directing agents as with encapsulation of silica nanoparticles the surface area reaches upto 229.5 m^2/g, confirms that the use of silica nanoparticles as structural directing agents are the best candidates for enhancing the surface area to many folds. The sorption isotherms of CuO/F-127, CuO/F-127/Dextran and CuO/F-127/TMB show rise when P/P^0 is above 0.8 or close to 1 (Fig. S2, A, B, C),[31] revealing the existence of macropores which is consistent with SEM results. The typical BJH pore size distributions of CuO/F-127, CuO/F-127/Dextran, CuO/F-127/TMB and CuO/F-127/Si-NPs were 8 µm, 780 nm, 830 nm and 39 nm respectively which is in complete agreement with the average pore diameter obtained from the SEM results, reveals the effect of structural directing agents.

Thermal gravimetric analysis (TGA)

The TGA curves of the as prepared samples were carried out before calcination (Fig. 4). The weight loss below 150 °C is due to the loss of physically absorbed water (3-15 %) [29,31,32] followed by 20-25 % weight loss at 150 °C-190 °C associated with decomposition of copper (II) nitrate to CuO.[2,3,30] The concomitant release of O_2 facilitated oxidative decomposition of Pluronic F-127/additives between 190 °C-395 °C with a considerable weight loss of 30-39 %.[30] Subsequently, between 395 °C and 410 °C, another mass loss of 3-4 % is measured, assigned to the combustion of remaining carbon species and left part of additives like TMB, dextran etc. The total weight loss during TGA process is 56-83 % and the left hybrid porous copper-oxide monoliths are 44-17 %.

FT-IR Study

The FT-IR spectra of as synthesized samples were carried out before calcination (Fig. 5). For the pure surfactant Pluronic F-127 (EO_{106} PO_{70} EO_{106}) the bands at 3400 cm^{-1}, 2890 cm^{-1}, 1370 cm^{-1} and 1050 cm^{-1} assigned to stretching vibrations of O – H, C – H, C – C and C – O, shifts to lower wavenumber as additives are introduced during the process of synthesis, confirms the complexation of Cu^{2+} cations by the EO groups of F-127 by a combination of electrostatic and hydrogen bonding interactions and forms ordered monoliths.[31] This pathway offers a promising alternative approach for introducing electrostatic forces and long range structural order into the assembly process while avoiding the need for acid concentrations i.e. green synthesis of porous materials (scheme 1).

Catalytic performance

It is well documented that dihydroxy phenols like catechol and hydroquinone are significant intermediates in agrochemical,[33] fine chemical industries[34] and have excellent pharmaceutical importance too,[33,34] thus a number of catalytic methods have been used to accomplish the hydroxylation of phenol to diphenols. Therefore, we used the hydroxylation of phenol to diphenols (catechol and hydroquinone) with oxidant H_2O_2 as a model system to quantitatively evaluate the catalytic performance of as synthesized series of porous copper oxide (CuO) monoliths at a particular reaction conditions, as the mechanism of conversion of phenol to diphenols is extremely sensitive to reaction conditions as well as quality of the catalyst.[34]

Possible mechanism

Several mechanisms have been reported for the hydroxylation of phenol with oxidant H_2O_2; most of them are based on free radicals, [35-37] though electrophilic mechanism has been noticed over titano silicates, [35] In the present study, an initial induction period was proposed in all cases in which porous CuO materials as a catalyst abstract H^+ ion from the phenol resulting in the formation of phenoxide ion. The produced phenoxide ion reacts with H_2O_2 resulting in the formation of diphenols and OH free radical. This OH free radical propagates the chain by attacking phenol molecule, forming diphenols. Same mechanism is proposed for formation of isomeric products also. The kinetic preference for catechol is explained by selective formation of hydroquinone inside the porous network of CuO monoliths.[34] The proposed mechanism is sketched in (Fig. 6)

From the experimental results as shown in Table 1, we find that porous CuO/F-127 as a catalyst has shown no conversion of phenol into diphenols (Catechol and hydroquinone) while as the unusual catalytic performance of mesoporous CuO monoliths (mpCuO) in the hydroxylation of phenol that might be because of specific surface area, availability of active sites on the catalyst, specific time period, catalyst concentration, and temperature.[34] Furthermore, the hydroxylation of phenol over the series of as-synthesized solid catalysts is heterogeneous type; mostly depend on the surface area of the catalyst [6-12,38] (Fig. 7).

A comparison of catalytic activity of mpCuO (CuO/F-127/Si-NPs) with the already reported catalysts to the best of my knowledge for the phenol hydroxylation by H_2O_2 is shown in Table 2. From the percentage (%) of phenol conversion values, we can see that activity of mesoporous CuO is higher than other reported catalysts. Therefore, mpCuO display promising potential applications in the phenol hydroxylation.

Electrochemical performance of mesoporous copper oxide monoliths

Precious metals (Platinum, gold) based catalysts are the excellent candidates for the fuel cell reactions and solar cell technology.[42] However, there are several drawbacks of using precious metal based catalysts like cost, very sensitive to contaminants, such as CO_2, H_2S, NH_3 and so on etc.[43] So, the use of non noble metal mesoporous materials as electrocatalysts in fuel cells as well as in solar cell technology are a subject of current interest in which mpCuO materials shows an interesting electrochemical performance in oxidative reductive reactions (ORR).[44-46] Herein, the electrocatalytic performance of as synthesized mesoporous copper oxide (CuO) monoliths as an electrocatalysts for ORR was investigated by electrochemical study. Fig. 8 (A) shows the cyclic voltammograms of mpCuO/GCE in 0.1M acetate buffer (pH 5) at a potential scan rate of 100 mVs^{-1}. It is interesting to note that the redox pair is attributed to the anodic oxidation of copper at 0.22 V and a reduction peak at - 0.14 V, suggesting the use of mpCuO nanostructures as building blocks in solar cell applications.

Furthermore, the mpCuO/GCE was used for analysis of p-nitrophenol where bare GCE in 0.1 M acetate buffer has shown no peak and at mpCuO/GCE produces a well distinct reduction peak at - 0.43V [Fig. 8 (B)] . It confirms that the reduction peak might be attributed to the reduction of p-nitrophenol.

This electrocatalytic behaviour of mesoporous CuO materials is attributed to its good conductivity, high specific surface area for loading p-nitrophenol and typical electronic structure (Fig. S3). Thus, allowing for the possibility of greater signals than what can’t be obtained with bare electrodes, demonstrating that the mesoporous CuO monoliths are excellent candidates for the fabrication of sensors for the determination of p-nitrophenol and other nitro phenols like o-nitrophenol and m- nitrophenol[47] which have significant industrial and pharmaceutical importance.

Conclusion

Hierarchically macro/mesostructured porous copper oxide monoliths have been successfully synthesized by simple, facile and environmentally benign Sol-Gel route with reliable control over shape, dimensionality, and crystallinity. The as synthesized porous copper oxide monoliths are well characterized to ascertain its catalytic activity for the first time towards the wet oxidation of phenol and electrochemical performance of mpCuO in the electrochemical reduction of p-nitrophenol originating from its unique porous nature. Such cost effective porous CuO materials can be expected to have a promising potential applications in biosensor fabrication, self-cleaning coating, electrocatalysts in alkaline fuel cells, electrochemical double layer supercapacitors and catalysts in organic synthesis.

Acknowledgement

The authors gratefully acknowledge UGC for financial assistance as Central University fellowship (CUF), Department of Chemistry, Dr. Hari Singh Gour Central University Sagar, (M.P) India, for providing the necessary facilities, Department of Chemistry, University of Mumbai for providing laboratory facilities for electrochemical study.

Notes and references

1. S. L. Brock, Science 2007, **317**, 460.
2. C. T. Kresge, M. E. Leonowicz, W. J. Roth, J. C. Vartuli and J. S. Beck, Nature, 1992, **359**, 710.
3. M. Hankel, Y. Jiao, A. Du, S. K. Gray and S. C. Smith, J. Phys. Chem. C, 2012, **116,** 6672.
4. W. C. E. Schofield, C. D. Bain and J. P. S. Badyal, Chem. Mater., 2012, **24,** 1645.
5. D. J. Fauth, M. L. Gray, H. W. Pennline, H. M. Krutka, S. Sjostrom and A. M. Ault, Energy Fuels, 2012, **26,** 2483.

6. C. Zapilko, Y. Liang, W. Nerdal and R. Anwander, Eur. J. Chem., 2007, **13,** 3169.
7. C. Shen, Y. J. Wang, J. H. Xu, K. Wang and G. S. Luo, Langmuir, 2012, **28,** 7519.
8. B. Y. Xia, W. T. Ng, H. B. Wu, X. Wang and X. W. Lou, Angew. Chem., Int. Ed. 2012, **51,** 7213.
9. X. W. Lou, L. A. Archer and Z. Yang, Adv. Mater., 2008 , **20,** 3987.
10. Z. Y. Wang, D. Luan, C. M. Li, F. B. Su, S. Madhavi, F. Boey and X. W. Lou, J. Am. Chem. Soc., 2010, **132,** 16271.
11. S. J. Ding, J. S. Chen, Z. Y. Wang, Y. L. Cheah, S. Madhavi, X. Hu and X. W. Lou, J. Mater. Chem., 2011, **21,** 1677.
12. L. Zhou, D. Y. Zhao and X. W. Lou, Angew. Chem., Int. Ed., 2012, **51,** 239.
13. F. Q. Sun, W. P. Cai, Y. Li, L. C. Jia and F. Lu, Adv. Mater., 2005, **17,** 2872.
14. M. D. Kim, S. A. Dergunov, E. Lindner and E. Pinkhassik, Anal. Chem., 2012, **84,** 2695.
15. Yoon et al., J. Electrochem. Soc., 2000, **147,** 2507
16. K. Liu et al., J. Electrochem. Soc., 1996, **143,** 124.
17. X.Y. lang et al. Scripta Materialia, 2011, **64,** 923
18. H.Liu et al ., J. Power Sources, 2007, **171,** 1054
19. J. A. Hubbell and R. Langer, Chem. Eng. News, 1995, **42,**
20. H.H. Tseng, I.A. Kumar, T.H. Weng, C.Y. Lu, M.Y. Wey, Desalination, 2009, **40,** 240.
21. Y. Li, W. P. Cai, B. Q. Cao, G. T. Duan, C. C. Li, F. Q. Sun and H. B. Zeng, J. Mater. Chem., 2006, **16,** 609.
22. F. Q. Sun, W. P. Cai, Y. Li, B. Q. Cao, Y. Lei and L. D. Zhang, Adv. Funct. Mater., 2004, **14,** 283.
23. J. S. Hu, L. L. Ren, Y. G. Guo, H. P. Liang, A. M. Cao, L. J. Wan and C. L. Bai, Angew. Chem., Int. Ed., 2005, **44,** 1269.

24. M. Jin, G. He, H. Zhang, J. Zeng, Z. Xie and Y. Xia, Angew. Chem., Int. Ed., 2011, **50,** 10560.

25. X. D. Wang, C. J. Summers and Z. L. Wang, Adv. Mater., 2004, **16,** 1215.

26. X. D. Wang, P. X. Gao, J. Li, C. J. Summers and Z. L. Wang, Adv. Mater., 2002, **14,** 1732.

27. Y. Li, W. Jia, Y. Song and X. Xia, Chem. Mater., 2007, **19,** 5758.

28. D. Walsh, I. Arceli, T. Ikoma, S. Tanaka, S. Mann, Nature Mater. 2003, **2,** 386.

29. F. Khan, M. Eswaramoorthy, C. N. R. Rao, Solid State Sci., 2007, **9,** 27.

30. F. Khan, S. Mann, J. Phys. Chem. C, 2009, **113,** 19871.

31. H. Zhang et al., J. Colloid interface sci., 2012, **380,** 16.

32. F. Kleitz, W. Schmidt, F. Schüth, Micropor. Mesopor. Mater., 2003, **65,** 1.

33. Gao. S.; Jia, X.; Yang, J.; Wei, X. J. Mater. Chem. 2012, **22,** 21733.

34. Kurian, M.; Sugunan, S. Chemical Engineering Journal 2006, **115,** 139.

35. H. Song, et al. J. Colloid interface Sci., 2011, **354,** 686.

36. R.Roy, C.H. Ko, M. Kruk, M. Antochshuk, J. Phys. Chem. B 2000, **104,** 11465

37. L.L.Lou, S. Liu, Catal. Commun., 2005, **6,** 762.

38. S.Gao, X. Jai, J. Yang, X. Wei, J. Mater. Chem., 2012, **22,** 21733

39. C.B.Liu et al. J. Catal., 1997, **168,** 35

40. G.Y. Zhang et al. Langmuir, 2006, **26,** 1362.

41. F.- S. Xiao et al., Appl. Catal. A 2001, **207,** 267.

42. S. Shu, G. Zhang, D. Geng, Y. Chen, R. Li, M. Cai and X. Sun, Angew. Chem., Int. Ed., 2011, **50,** 422.

43. M. Nosonovsky and B. Bhushan, Microsyst. Technol., 2005, **11,** 535.

44. G. T. Cheek and W. E. O’Grady, J. Electroanal. Chem., 1995, **385,** 45.

45. Dutta, M. K. Carpenter, M. P. Balogh, J. M. Ziegelbauer, T. E. Moylan, M. H. Atwan and N. P. Irish, J. Phys. Chem. C, 2010, **114,** 16309.

46. F. R. Brushett, M. S. Thorum, N. S. Lioutas, M. S. Naughton, C. Tornow, H. M. Jhong, A. A. Gewirth and P. J. A. Kenis, J. Am. Chem. Soc., 2010, **132,** 12185.

47. Liu Z.N. et al., Electrochem. Commun., 2009, **11,** 1365.

Figure captions

Fig. 1 PXRD patterns of porous copper-oxide monoliths prepared using F-127 as a reducing agent (A-D). Porous CuO monoliths prepared by calcination of (A) copper nitrate/F-127, (B) copper nitrate/F-127/dextran, (C) copper nitrate/F-127/TMB (D) copper nitrate/F-127/silica nanoparticles.

Fig. 2 SEM micrographs of porous copper oxide scaffolds synthesized using F-127 as a non-ionic surfactant. Monoliths were prepared by calcination of (A), copper nitrate/F-127 gel , showing average pore diameter of 9.5 µm; scale bar = 50 µm, (B) copper nitrate /F -127/ dextran gel, with average pore diameter 780 nm; scale bar = 5 µm, (C) copper nitrate/F-127/TMB, showing average pore diameter of 830 nm; scale bar = 5 µm, (D) copper nitrate/ F-127/Si-NPs gel, with average pore diameter of 39 nm; scale bar = 200 nm.

Fig. 3 Nitrogen sorption isotherm for mesoporous copper oxide (mpCuO) monoliths prepared by the calcination of copper nitrate/F-127/Si-NPs gel. The inset shows the pore size distribution.

Fig. 4 (a) TGA profiles of copper nitrate/F-127 xerogels with and without additives were carried out before calcination. (A) copper nitrate/F-127, (B) copper nitrate/F-127/Dextran, (C) copper nitrate/F-127/TMB, (D) copper nitrate/F-127/Si-NPs. **(b)** 3D view of the same thermogram with symbols corresponding the same samples.

Fig. 5 Fourier Transform Infrared spectroscopic (FT-IR) studies of porous CuO xerogels carried out before calcination. (A) Pure Pluronic F-127, (B) copper nitrate/F-127, (C) copper nitrate/F-127/dextran (D) copper nitrate/F-127/TMB, (E) copper nitrate/F-127/Si-NPs.

Fig. 6 Plausible mechanism of wet oxidation of phenol with oxidant H_20_2

Fig. 7 Graphical representation of catalytic activity of porous CuO monoliths showing heterogenous catalytic reactions depends on the surface area.

Fig. 8 (A) The cyclic voltammograms of mesoporous copper oxide modified glassy carbon electrode (mpCuO/GCE) in 0.1M acetate buffer (pH 5). (a) Bare GCE and (b) mpCuO/GCE at a scan rate of $100mVs^{-1}$. **(B)** Differential pulse voltammograms (DPV) of $0.1x10^{-6}$M p-nitrophenol in 0.1M acetate buffer (pH 5) at (a) Bare GCE and (b) mpCuO/GCE at scan rate of 100 mVs.

Fig. S1 EDAX analysis of CuO/F-127/Si-NPs

Fig. S2 (A) Nitrogen sorption isotherm for macroporous copper oxide monoliths prepared by the calcination of copper nitrate/F-127 gel

Fig. S2 (B) Nitrogen sorption isotherm for macroporous copper oxide monoliths prepared by the calcination of copper nitrate/F-127/Dextran gel

Fig. S2 (C) Nitrogen sorption isotherm for macroporous copper oxide monoliths prepared by the calcination of copper nitrate/F-127/TMB gel

Fig. S3 Typical electronic structure of porous copper oxide monoliths showing a covalent bonding interaction between Cu-O

Scheme 1 (a) $Cu(NO_3)_2 .3H_2O$ solution mixed with (b) Pluronic F-127 solution with and without additives. (c) Light blue colour solution formed (SOL). (d) Heat cum magnetic stirring at $55^{O}C$ followed by ageing for 2-3 days resulting into cross linking of precursor with F-127 (GEL formation). (e) Calcination of the resulting gel at 650 °C results into porous copper oxide monoliths.

Tables

Table 1 Catalytic activity in phenol hydroxylation by H_2O_2 over a series of porous copper oxide monoliths as catalysts. [a]

Catalysts	BET Surface area (m^2/g)	pore volume (cm^3/g)	Conversion (%)	Product Selectivity			Yield (%)
				Catechol	Hydroquinone	Diphenol	
CuO/F-127	0.558	0.00038	----	----	----	----	----
CuO/F-127/Dextran	19.72	0.02967	13.20	21.01	5.02	26.03	3.44
CuO/F-127/TMB	25.94	0.04915	17.36	29.07	14.30	43.37	7.52
CuO/F-127/Si-Nps	229.5	0.32715	91.01	71.05	19.16	90.21	82.10

[a] Reaction conditions: Phenol: 1.0 g; phenol / H_2O_2 (molar ratio): 1:1; Catalyst: 50 mg; solvent (water): 17.5 ml; reaction temperature 50 °C; time 3.5 h.

Table 2 Comparison of catalytic performance in the phenol hydroxylation by H_2O_2 over different catalysts.

Catalysts	Conversion (%)	Product selectivity			Yield (%)	References
		Catechol	Hydroquinone	Diphenol		
CuO/F-127/Si-NPs [a]	91.01	71.05	19.16	90.21	82.10	This work
Fe^{2+} (Fenton reagent) [b]	20.5	68.7	18.9	87.6	17.95	Ref.39
Cu/MCM-41-M [c]	4.2	40.1	19.2	59.3	2.40	Ref.40
Cu/MCM-41-H [c]	25.0	39.9	23.0	62.9	15.72	Ref.40
Cucl$_2$ [d]	7.5	39.6	35.3	74.9	5.60	Ref.41

[a] Reaction conditions: Phenol: 1.0 g; phenol / H_2O_2 (molar ratio): 1:1; Catalyst: 50 mg; solvent (water): 17.5 ml; reaction temperature 50 °C; time 3.5 h.

[b] Reaction conditions (40): Reaction time: 6 h; temperature: 50 °C; reaction medium: water; pH 7.0; concentration of phenol: 0.35 mol/l; molar ratio phenol/H_2O_2: 1.0; volume of reacting mixture: 15 ml.

[c] Reaction conditions (41): phenol: 1.0 g; phenol/ H_2O_2 (molar ratio): 1.0; catalyst: 50 mg; solvent (water): 20 ml; temperature: 60 °C; time 6 h.

[d] Reaction conditions (42): phenol: 17 mmol; phenol/ H_2O_2 (molar ratio): 3.0; catalyst/phenol: (molar ratio): 0.02; reaction time: 4 h, reaction temperature: 80 °C.

Graphical abstract

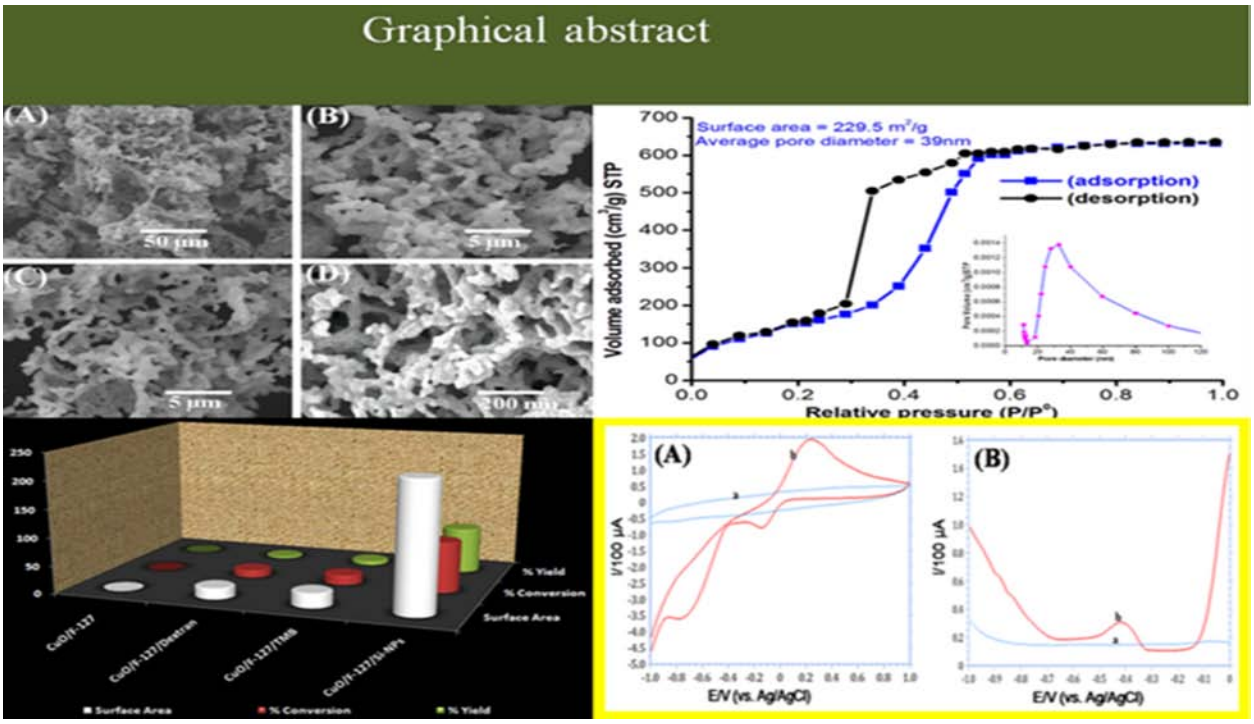

Figures

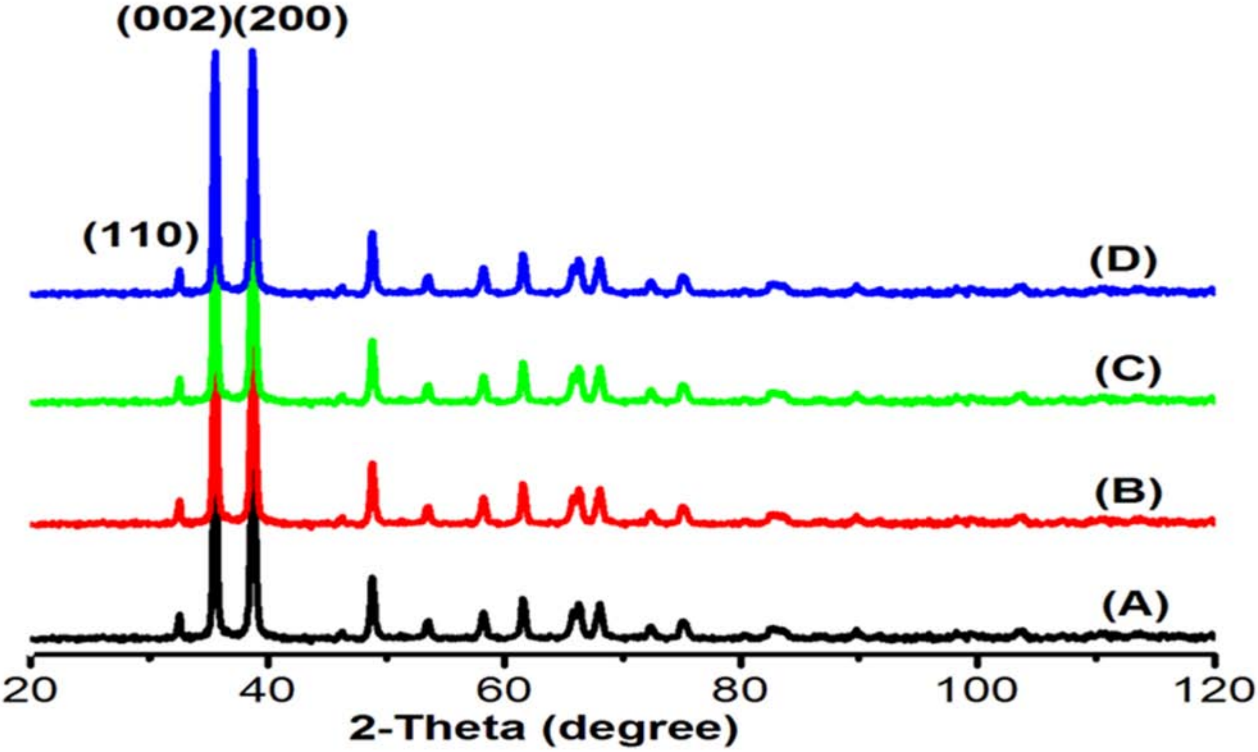

Fig. 1

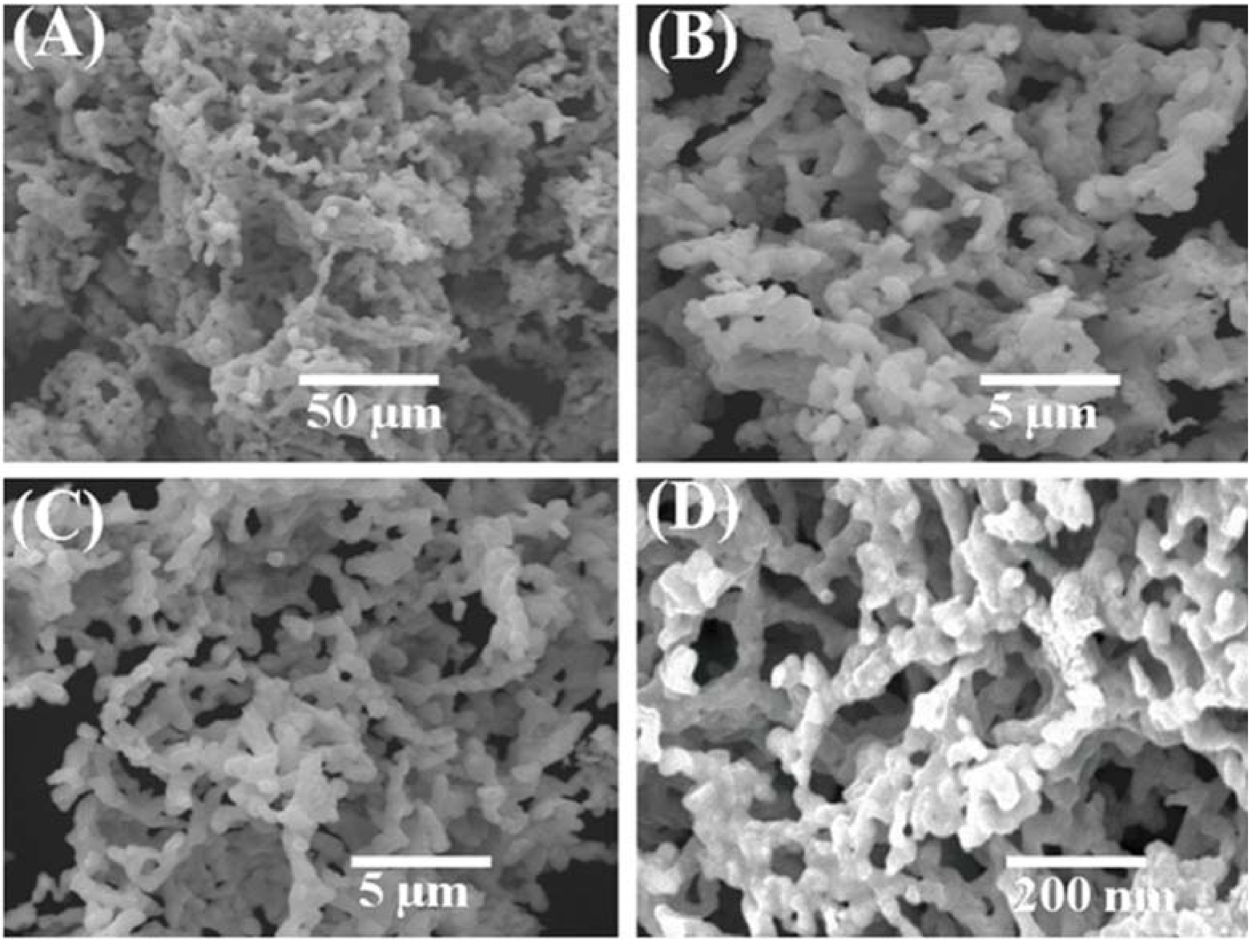

Fig. 2

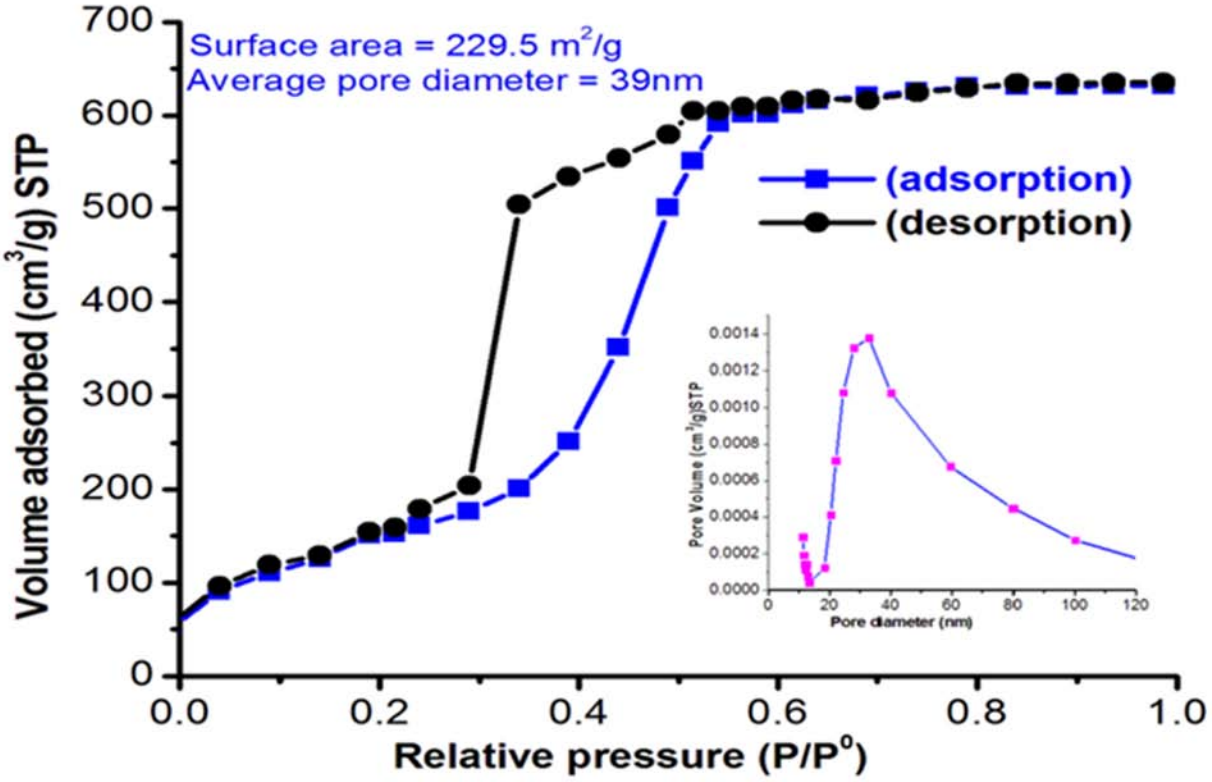
Surface area = 229.5 m^2/g
Average pore diameter = 39nm
(adsorption)
(desorption)
Volume adsorbed (cm^3/g) STP
Relative pressure (P/P^0)
0
100
200
300
400
500
600
700
0.0
0.2
0.4
0.6
0.8
1.0
Pore Volume (cm^3/g)STP
Pore diameter (nm)
0.0000
0.0002
0.0004
0.0006
0.0008
0.0010
0.0012
0.0014
0
20
40
60
80
100
120

Fig. 3

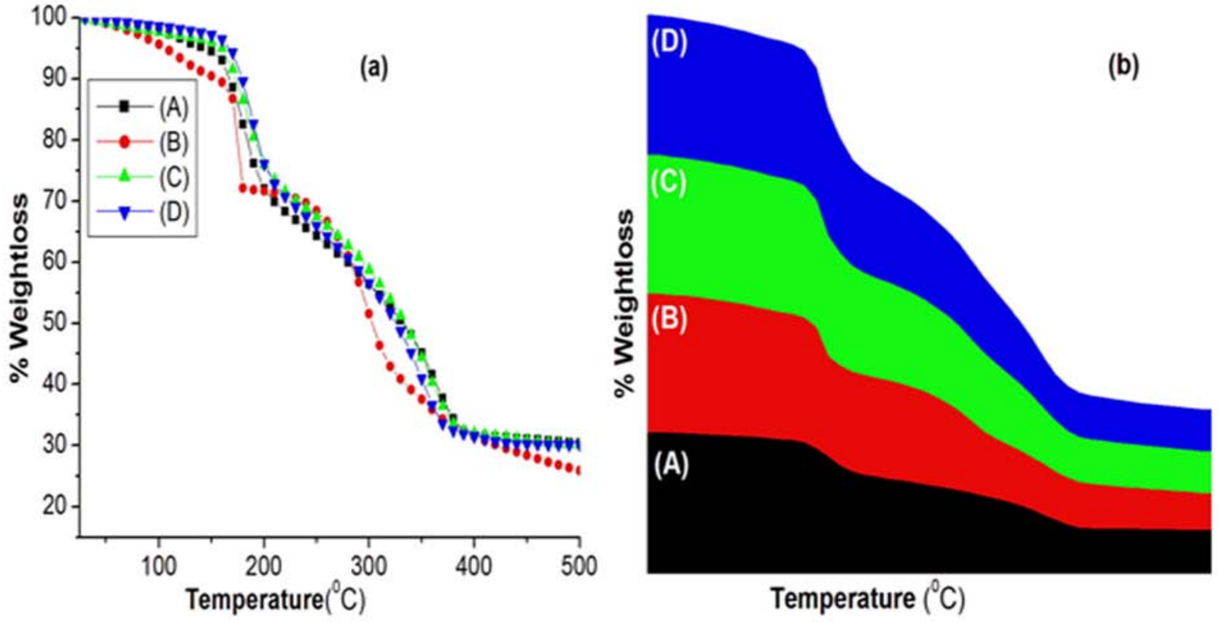
100
90
80
70
60
50
40
30
20
% Weightloss
(a)
(A)
(B)
(C)
(D)
100
200
300
400
500
Temperature(°C)
(b)
% Weightloss
(D)
(C)
(B)
(A)
Temperature (°C)

Fig. 4

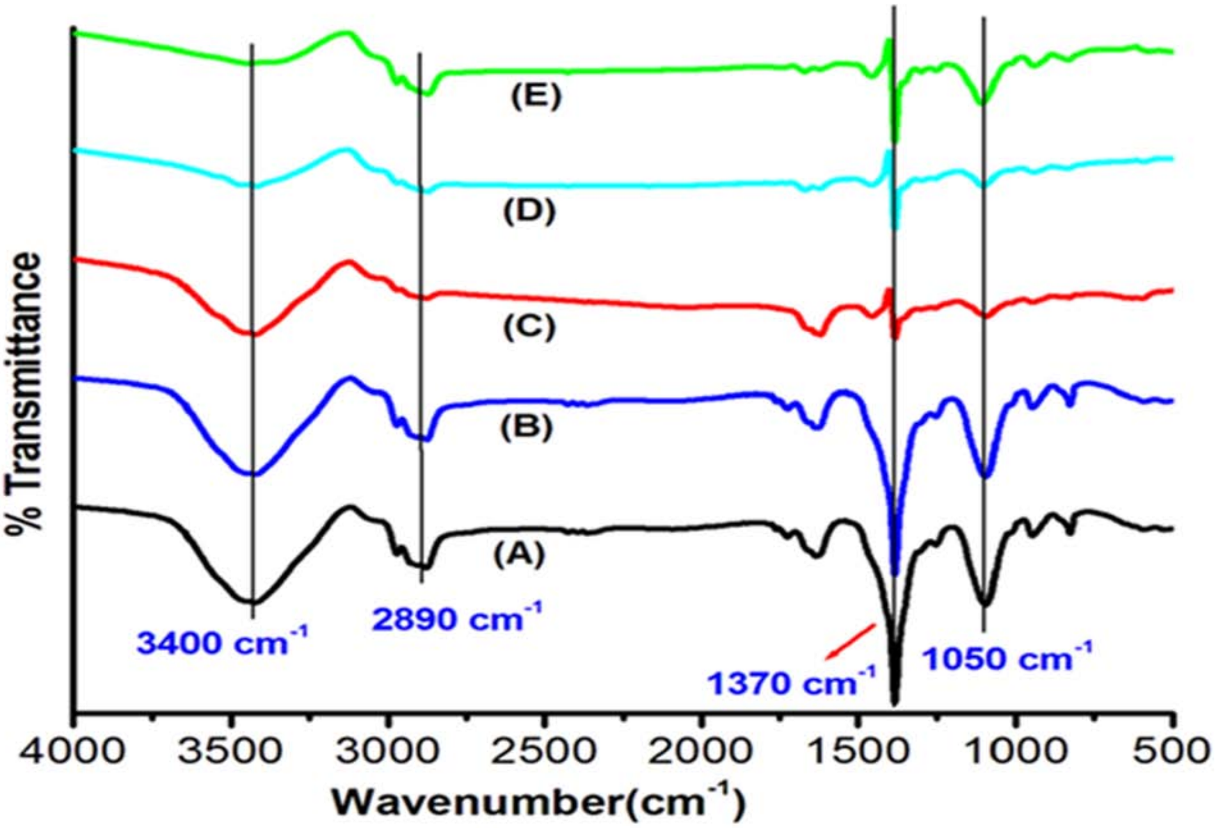
(E)
(D)
(C)
(B)
(A)
% Transmittance
3400 cm-1
2890 cm-1
1370 cm-1
1050 cm-1
4000
3500
3000
2500
2000
1500
1000
500
Wavenumber(cm-1)

Fig. 5

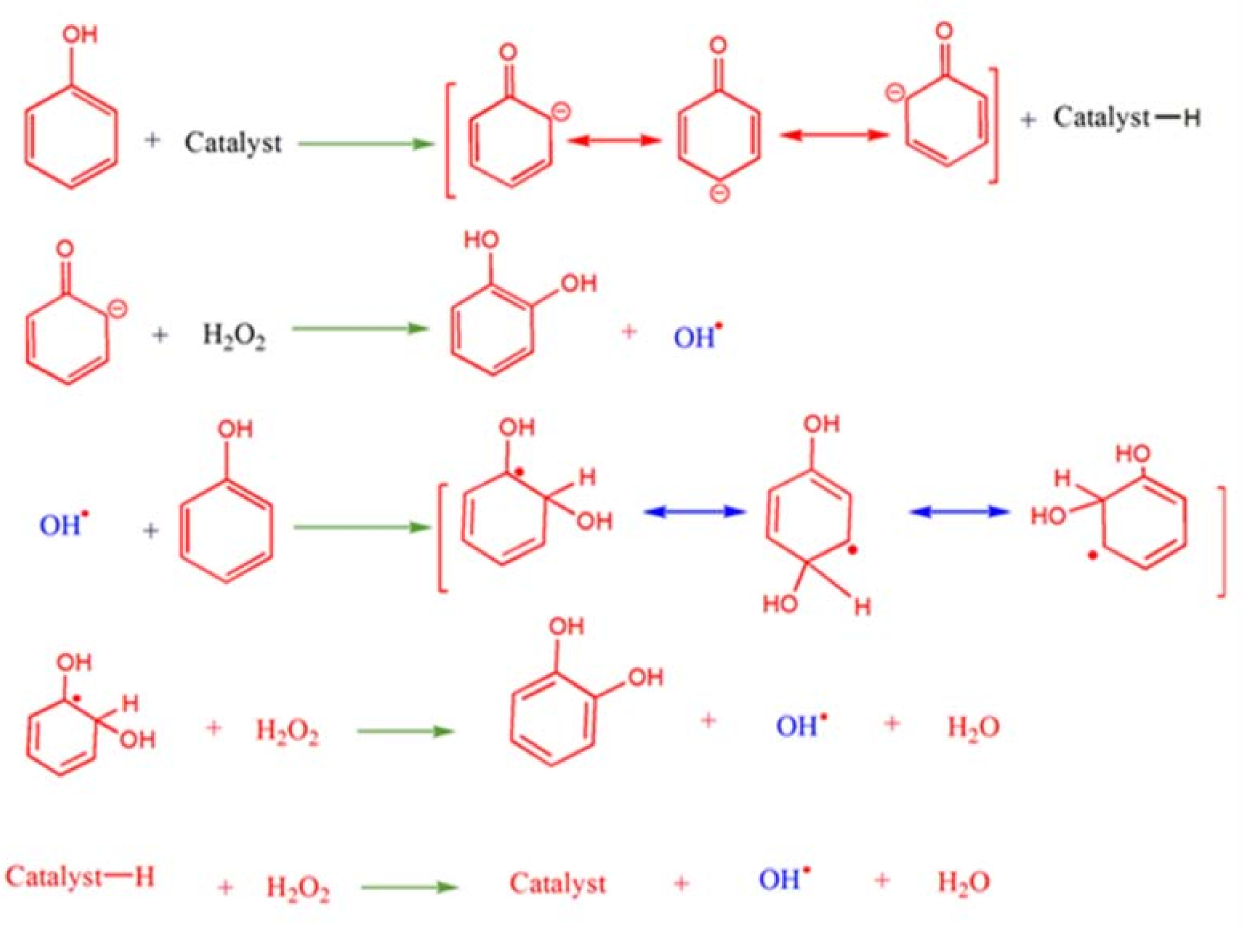
OH
+ Catalyst
O
O
O
+ Catalyst—H
O
+ H_2O_2
HO
OH
+ $OH^\bullet$
$OH^\bullet$
+
OH
OH
H
OH
OH
HO
H
H
HO
HO
OH
H
OH
+ H_2O_2
OH
OH
+ $OH^\bullet$
+ H_2O
Catalyst—H
+ H_2O_2
Catalyst
+ $OH^\bullet$
+ H_2O

Fig. 6

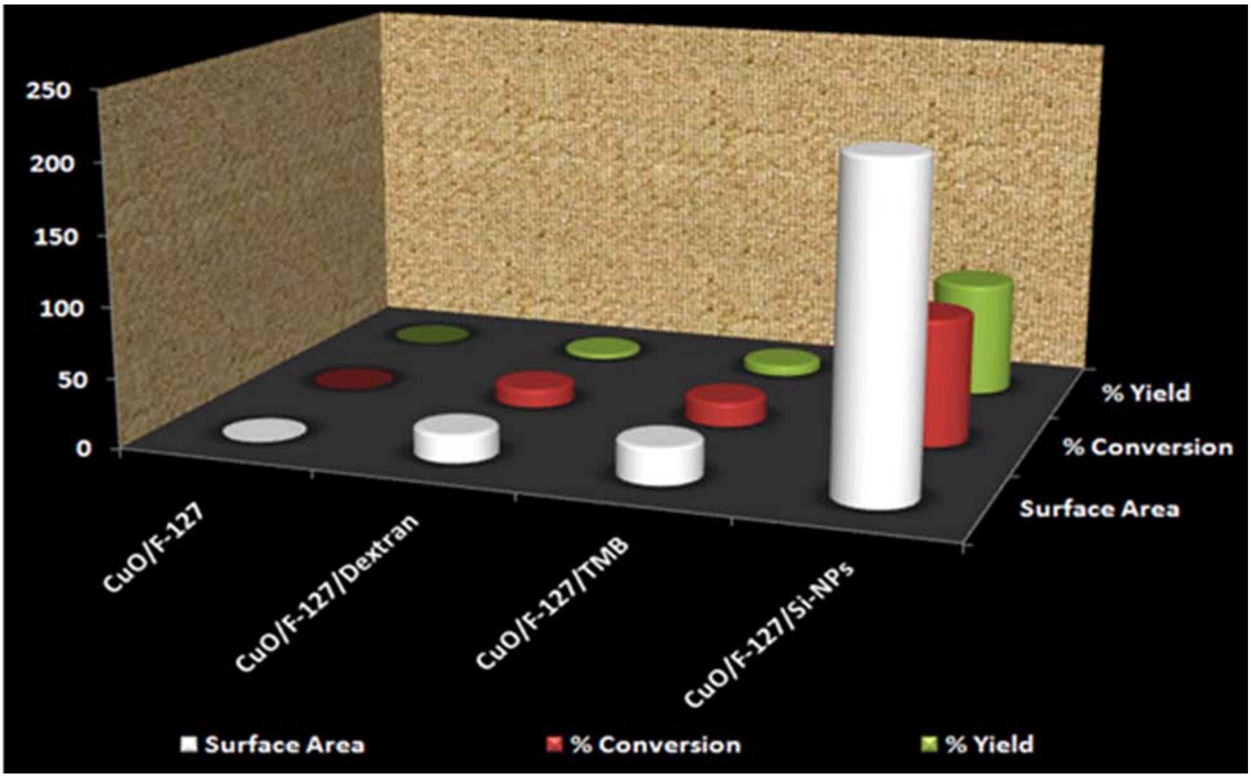
250
200
150
100
50
0
CuO/F-127
CuO/F-127/Dextran
CuO/F-127/TMB
CuO/F-127/Si-NPs
% Yield
% Conversion
Surface Area
Surface Area
% Conversion
% Yield

Fig. 7

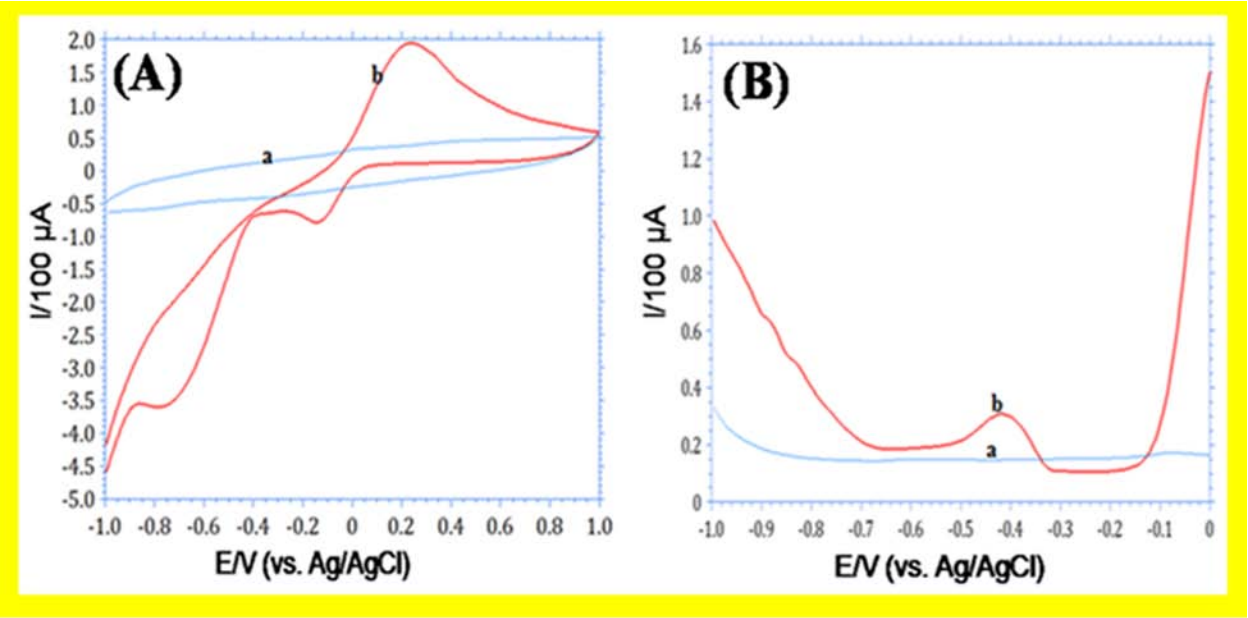
(A)
b
a
2.0
1.5
1.0
0.5
0
-0.5
-1.0
-1.5
-2.0
-2.5
-3.0
-3.5
-4.0
-4.5
-5.0
I/100 µA
-1.0
-0.8
-0.6
-0.4
-0.2
0
0.2
0.4
0.6
0.8
1.0
E/V (vs. Ag/AgCl)
(B)
b
a
1.6
1.4
1.2
1.0
0.8
0.6
0.4
0.2
0
I/100 µA
-1.0
-0.9
-0.8
-0.7
-0.6
-0.5
-0.4
-0.3
-0.2
-0.1
0
E/V (vs. Ag/AgCl)

Fig. 8

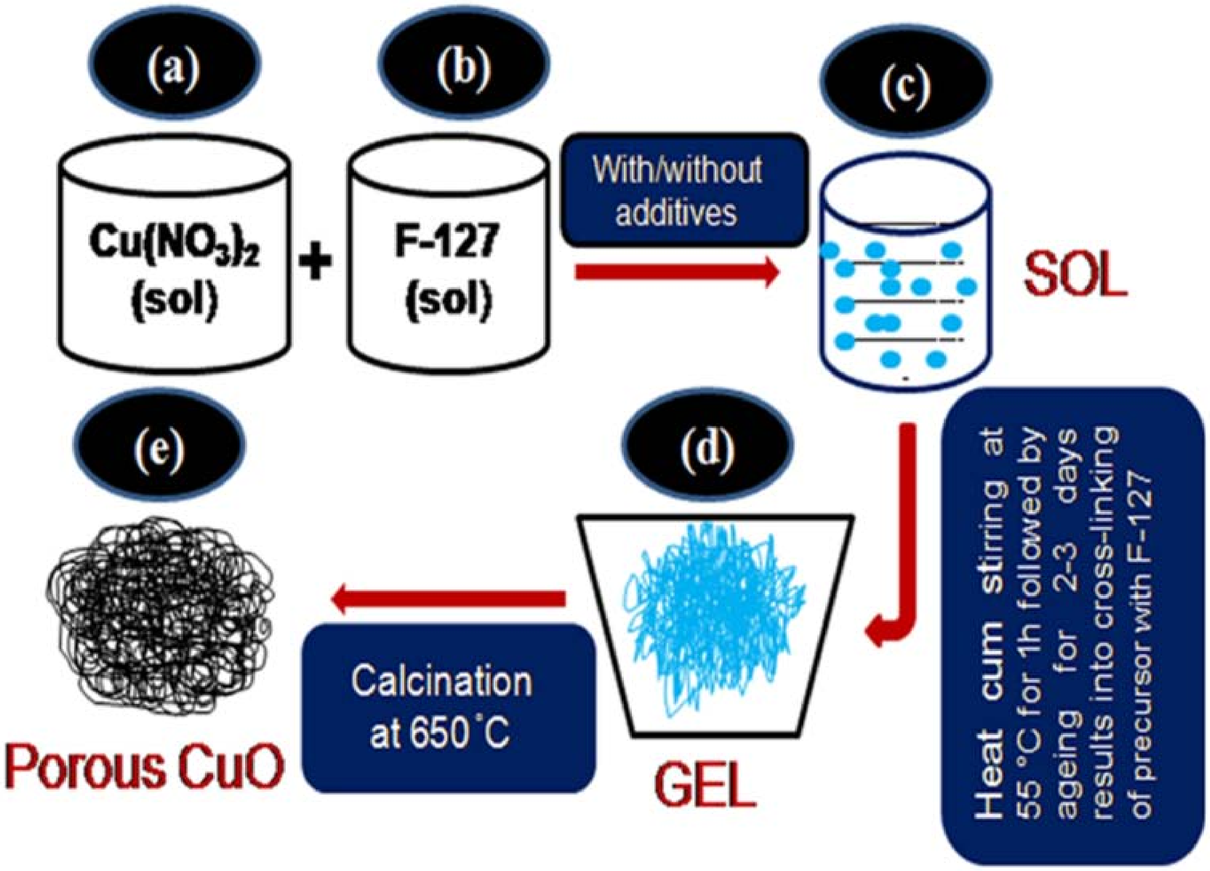
(a)
$Cu(NO_3)_2$ (sol)
+
(b)
F-127 (sol)
With/without additives
(c)
SOL
Heat cum stirring at 55 °C for 1h followed by ageing for 2-3 days results into cross-linking of precursor with F-127
(d)
GEL
Calcination at 650˚C
(e)
Porous CuO

Scheme 1

Supplementary data

Hierarchically macro/mesostructured porous copper oxide: Facile synthesis, Characterization, Catalytic performance and Electrochemical study of mesoporous copper oxide monoliths

Gowhar Ahmad Naikoo,[a] Riyaz Ahmad Dar [b] and Farid Khan *[a]

[a]Nanomaterials discovery laboratory,
Department of chemistry,
Dr. Hari Singh Gour Central University, Sagar (M.P) 470003, India.
[b]Department of Chemistry,
University of Mumbai, Vidyanagari Santacruz (East)-Mumbai-400098, India
Email id:-faridkhan58@yahoo.com
Tel: +91-9425626334

Corresponding author: - Farid khan

Designation: - Professor

Email id:-faridkhan58@yahoo.com

Phone: - +91-9425626334

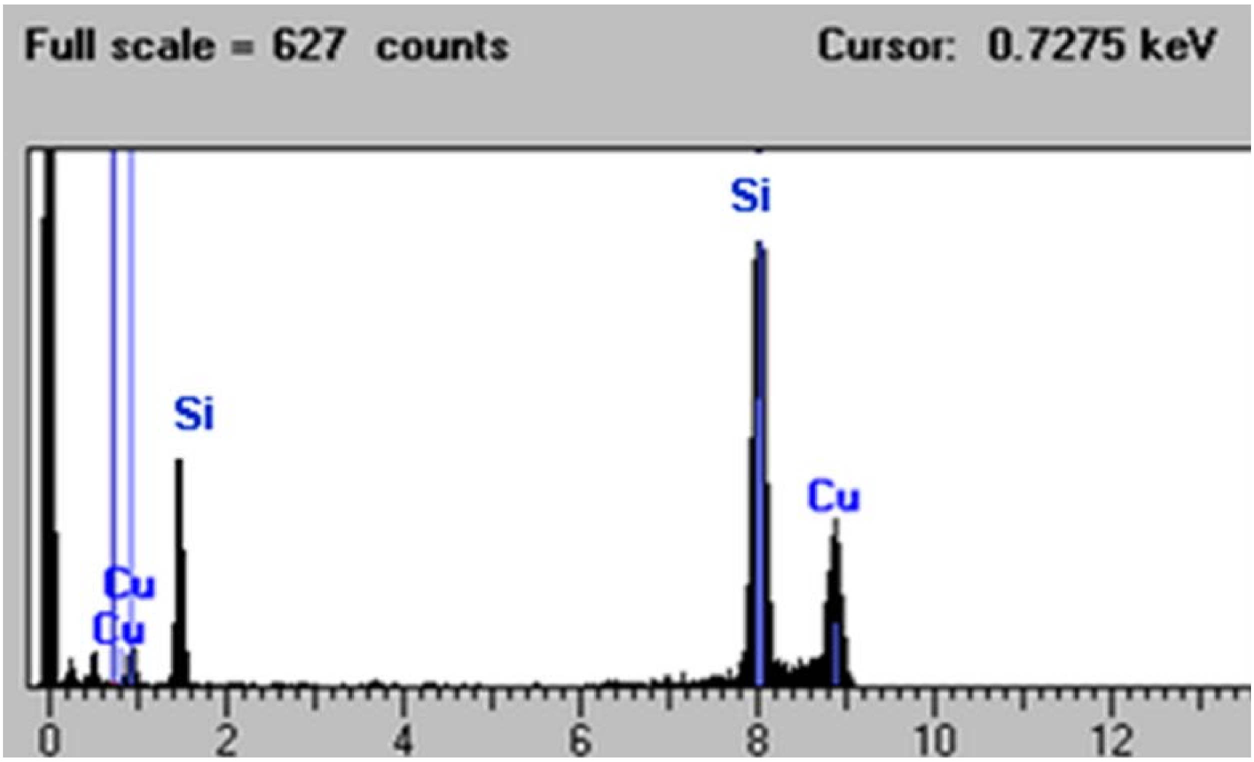
Full scale = 627 counts
Cursor: 0.7275 keV
Si
Si
Cu
Cu
Cu
0
2
4
6
8
10
12

Fig. S1

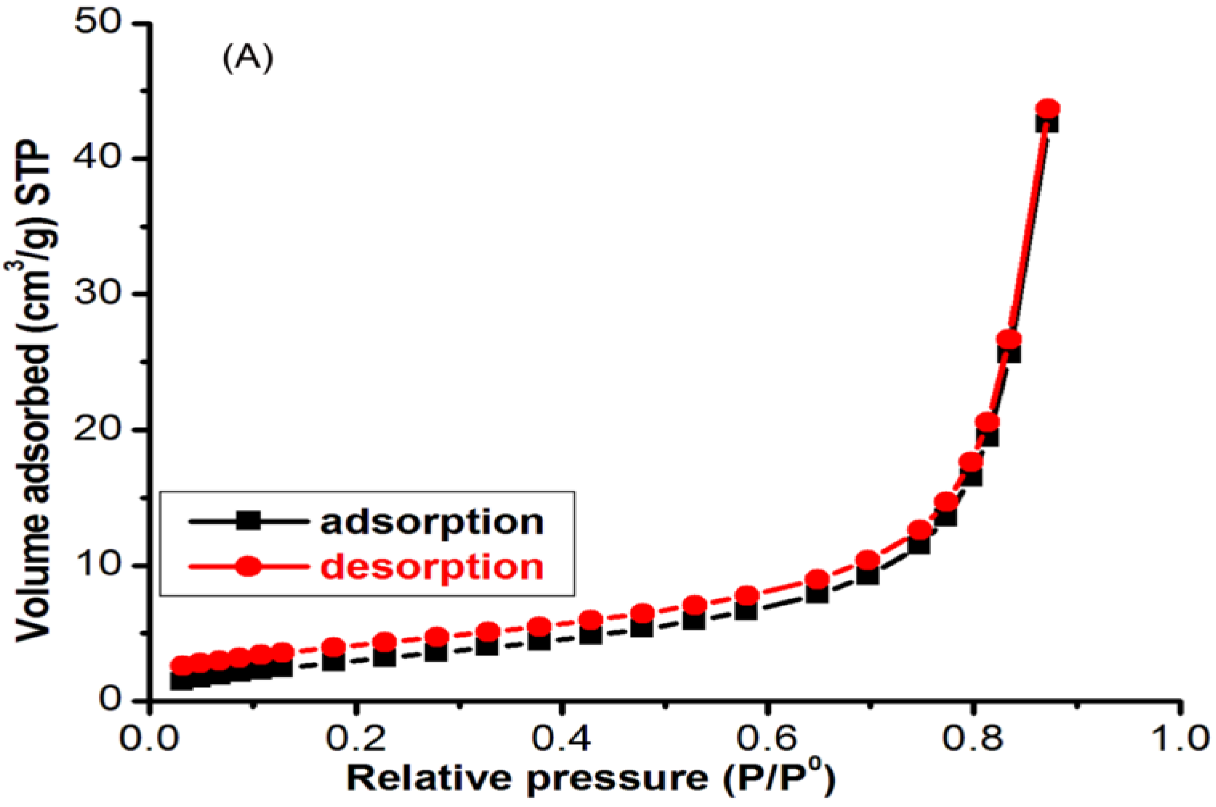
(A)
Volume adsorbed (cm^3/g) STP
0
10
20
30
40
50
Relative pressure (P/P^0)
0.0
0.2
0.4
0.6
0.8
1.0
adsorption
desorption

Fig.S2 (A)

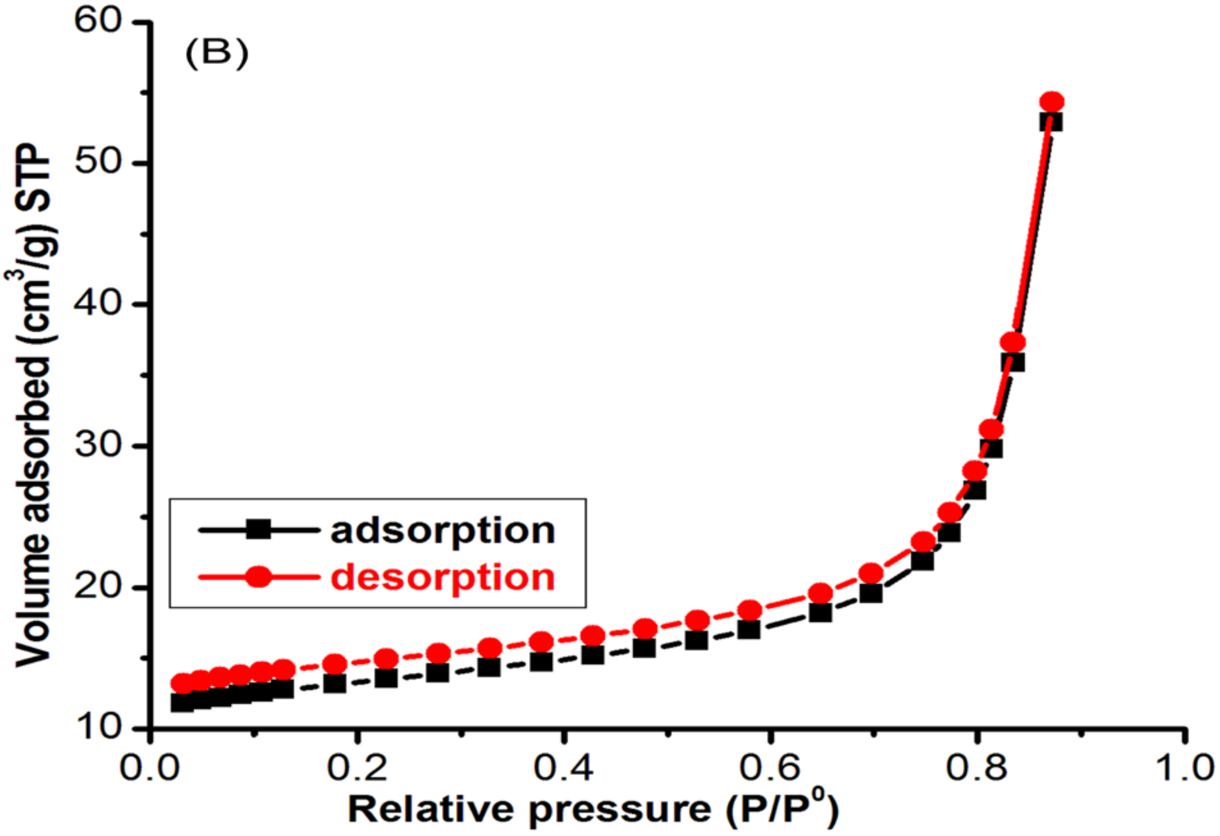
(B)
Volume adsorbed (cm^3/g) STP
Relative pressure (P/P^0)
adsorption
desorption
10
20
30
40
50
60
0.0
0.2
0.4
0.6
0.8
1.0

Fig. S2 (B)

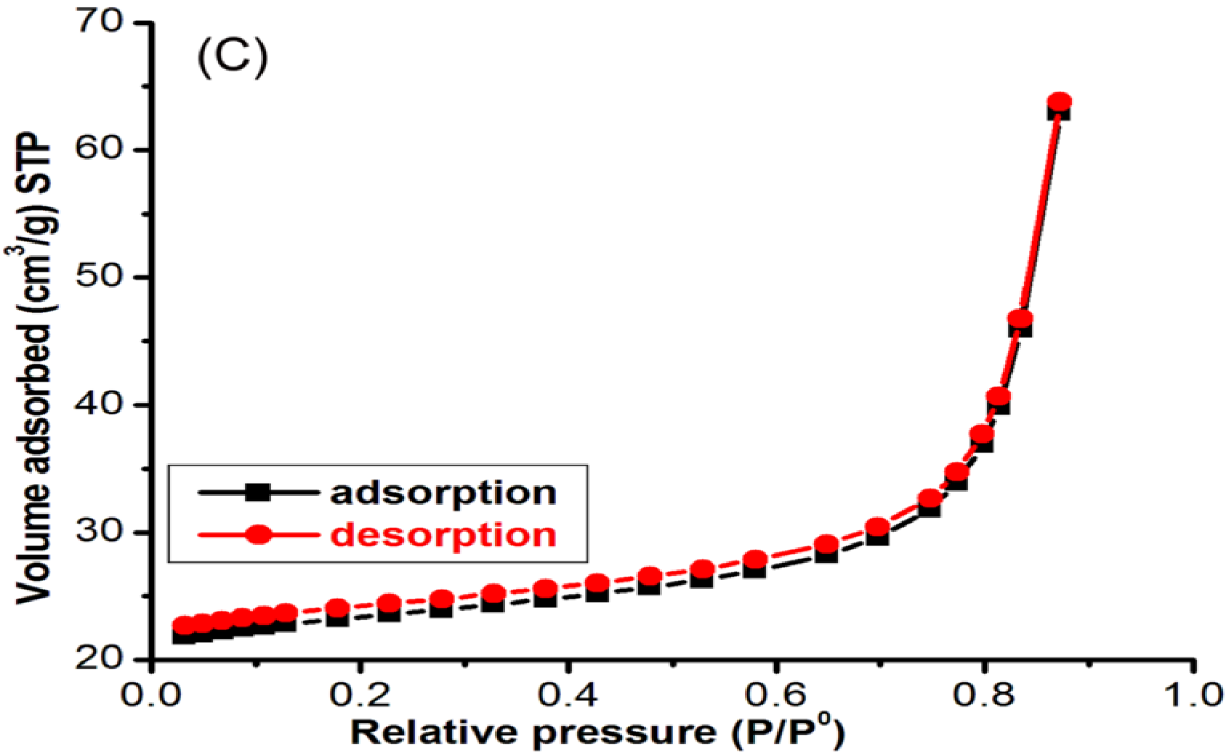
(C)
Volume adsorbed (cm^3/g) STP
70
60
50
40
30
20
0.0
0.2
0.4
0.6
0.8
1.0
Relative pressure (P/P^0)
adsorption
desorption

Fig. S2 (C)

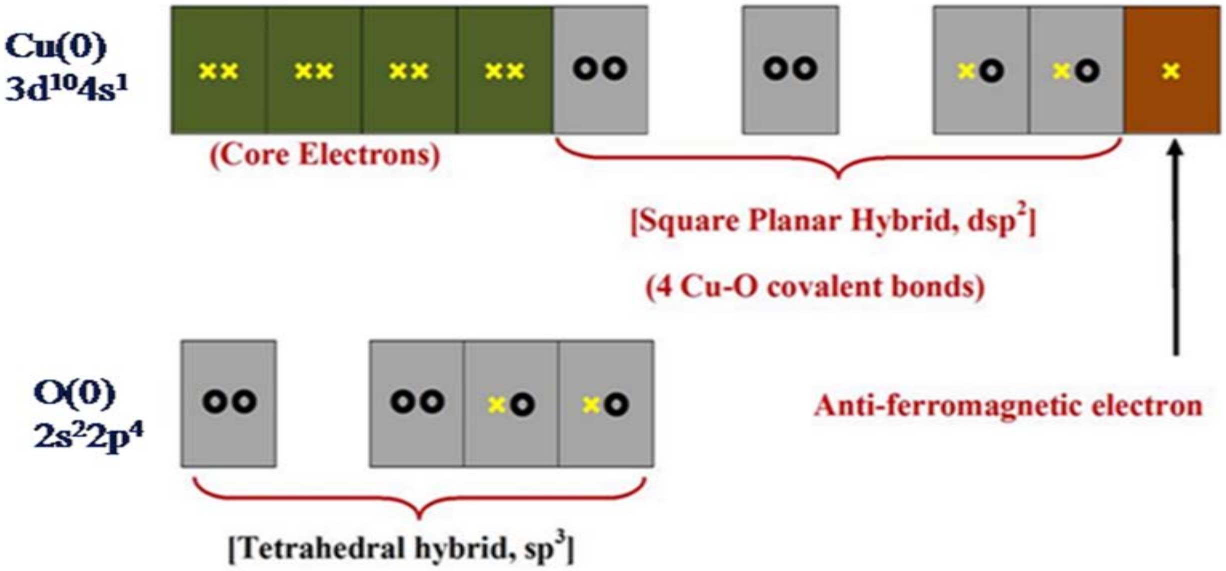
Cu(0)
3d¹⁰4s¹
(Core Electrons)
[Square Planar Hybrid, dsp²]
(4 Cu-O covalent bonds)
Anti-ferromagnetic electron
O(0)
2s²2p⁴
[Tetrahedral hybrid, sp³]

Fig. S3